Retinal Microvascular Impairment in the Early Stages of Parkinson's Disease

William Robert Kwapong,[1] Hua Ye,[2] Chenlei Peng,[1] Xiran Zhuang,[1] Jianhua Wang,[3] Meixiao Shen,[1] and Fan Lu[1]

[1]School of Ophthalmology and Optometry, Wenzhou Medical University, Wenzhou, Zhejiang, China
[2]The Neurology Department, Wenzhou Peoples' Hospital, Wenzhou, Zhejiang, China
[3]Department of Ophthalmology, Bascom Palmer Eye Institute, University of Miami, Miami, Florida, United States

Correspondence: Meixiao Shen, School of Ophthalmology and Optometry, Wenzhou Medical University, 270 Xueyuan Road, Wenzhou, Zhejiang 325027, China; shenmxiao7@hotmail.com.
Fan Lu, School of Ophthalmology and Optometry, Wenzhou Medical University, 270 Xueyuan Road, Wenzhou, Zhejiang 325027, China; lufan62@mail.eye.ac.cn.

WRK and HY contributed equally to the work presented here and should therefore be regarded as equivalent authors

Submitted: October 26, 2017
Accepted: April 25, 2018

Citation: Kwapong WR, Ye H, Peng C, et al. Retinal microvascular impairment in the early stages of Parkinson's disease. *Invest Ophthalmol Vis Sci*. 2018;59:4115–4122. https://doi.org/10.1167/iovs.17-23230

Purpose. To detect the retinal microvascular impairment using optical coherence tomography angiography (OCT-A) in patients with Parkinson's disease (PD) and find a correlation between the microvascular impairment and the neuronal damage.

Methods. This is a prospective, observational study including 49 eyes from 38 PD patients in their early stages and 34 eyes from 28 healthy controls with comparable age range. Macula microvasculature was evaluated with the spectral-domain optical coherence tomography (SD-OCT) angiography and intraretinal layer thickness evaluated with the SD-OCT. A custom algorithm was used for custom segmentation of retinal thickness and quantification of the superficial and deep microvascular density of the macula, respectively.

Results. PD patients showed reduced microvascular density in most of the areas of the whole retina. In the superficial retinal capillary plexus, statistical difference ($P < 0.01$) was seen in the total annular zone (TAZ), superior, temporal, inferior, and nasal zones. In PD patients, there was a strong correlation between the average ganglion cell layer and inner plexiform (GCIP) thickness and the TAZ of the superficial microvascular density ($r = 0.062$, $P = 0.032$).

Conclusion. We demonstrated that retinal microvascular density decreased in PD patients. The correlation between microvascular impairment in the superficial retinal capillary layer and GCIP thinning also revealed that the retinal microvascular abnormality may contribute to the neurodegeneration in PD patients. OCT-A with quantitative analysis offers a new path of study and will likely be useful in the future as an objective biomarker for detecting vessel impairment in early stages of PD.

Keywords: Parkinson's disease, optical coherence tomographic angiography, retinal microvasculature

Parkinson's disease (PD), the second most common neurodegenerative condition in the aging human population, is known to cause irreversible deterioration in cognitive function secondary to neuronal cell death and brain atrophy.[1] The main cause of disability in patients with PD is the loss of dopaminergic neurons in the central nervous system.[2,3] Dopamine, which serves a vital role for visual processing in the retina, has been reported to be deficient in the retina of patients with PD.[4] Visual symptoms, such as decreased visual acuity, visual hallucinations, and deficits in visuospatial orientation, have been commonly reported in patients with PD.[5–7]

Neuronal degeneration in PD has been well documented in human cases, providing fundamental information for the establishment of animal models and their use of drug discovery and the development of these conditions. In addition to neurodegeneration, the vascular component in PD has been identified as a key pathological feature and a possible contributing factor to the disease occurrence and progress.[8,9] Therefore, surrogate clinical markers are needed to quantify the early vascular abnormality of PD that would allow treatment to begin in the early stages of the disease that may help forestall its development or provide restoration of damaged neural systems.

The effect of PD on the microvascular components of the brain is generally difficult to examine directly.[10] With the retina being a window to the brain, it possesses the unique advantage in which neurodegenerative diseases are correlated with the structural changes in the neurons and microvessels.[11] Thus, it provides the opportunity to detect and directly monitor changes in the neuronal and microvessels of neurodegenerative diseases such as PD and Alzheimer's disease. Optical coherence tomography (OCT) is a noninvasive procedure used for the analysis of retinal morphology. It has been effectively used to assess disease progression in patients with neurodegenerative conditions such as multiple sclerosis.[12,13] OCT has been suggested as a surrogate measure for brain damage in some systemic diseases, such as migraine.[14] Since the early description of impaired visual processing in PD, an increasing number of articles have been published using OCT to document the structural changes of the retina in PD patients.[4,15–17] Comparatively, the study of vessel changes in the retina in PD has received less attention due to the lack of suitable modality to image the microvascular network in vivo. In recent years, OCT angiography (OCT-A) was extended based on OCT technology, which can be used to characterize the three-dimensional (3D) vasculature in various retinal layers, providing quantitative

assessment of the microvascular and morphological structure in the retina. The current study was performed to determine the retinal microvascular changes that occur in the early stages of PD patients using OCT-A and their correlation with the retinal structural changes.

Methods

Patients with confirmed idiopathic PD diagnosis were included in this observational cross-sectional study. A total of 44 patients and 30 healthy individuals were evaluated. All procedures adhered to the tenets of the Declaration of Helsinki and were approved by the Ethics Committee of the Eye Hospital of Wenzhou Medical University, Wenzhou, China. All participants provided written informed consent to participate in the study.

The diagnosis of PD was made by a single neurologist (HY) based on the UK Brain Bank Criteria,[18] and information about the disease severity (using the Hoehn and Yahr [H&Y] scale),[19] disease duration, and treatment was recorded. All subjects underwent a complete ophthalmological evaluation, including visual acuity measured with the Snellen chart, slit-lamp biomicroscopy, IOP measurement, funduscopic examination, and OCT imaging. Refraction was assessed in all subjects and patients with significant refractive errors (>5 diopters [D] of spherical equivalent refraction or 3D of astigmatism) were excluded. Observable ocular changes during the ophthalmological evaluation, such as retinal changes associated with high myopia, were excluded from the study. Other exclusion criteria were IOP ≥21 mm Hg, media opacifications, concomitant ocular diseases (including history of glaucoma or retinal pathology), and systemic conditions that could affect the visual system, such as diabetes, uncontrolled hypertension/hypotension, history of cardiac diseases, neurological diseases such as multiple sclerosis, and peripheral nerve diseases by other processes different from PD were excluded from the study. Eyes with suspicion of glaucomatous damage were also excluded from the study. Individuals with previous ocular surgery that could affect the visual outcomes or the macular morphology were also excluded from the study. Subjects with similar age range from the working staff of the Eye Hospital, Wenzhou Medical University, Wenzhou, China, served as healthy controls. The healthy individuals were carefully examined and met the same exclusion criteria as patients. They had no history or evidence of ocular, neurological, or systemic disease of any nature.

Retinal Capillary Imaged by SD-OCT-A

Retinal microvasculature was also imaged by the RTVue XR Avanti Spectral-Domain OCT system (Optovue, Inc., Fremont, CA, USA) equipped with AngioVue software (Version 2015.1.0.90).[20] The eye movement was offset during image processing using the Motion Correction Technology function. The scan speed was 70,000 A-scans per second and the scan area, centered on the fovea was 3 × 3 mm^2, obtained by orthogonal registration and merging of two consecutive scans. The size of the exported OCT images was 304 × 304 pixels. A good set of scans, with a signal strength index (SSI) of >40 for each eye, was selected for further analysis. Any image with double vessel pattern or motion artifacts of more than three lines was excluded. The superficial retinal capillary plexus (SRCP) and deep retinal capillary plexus (DRCP) were detected and separated automatically by the OCT instrument. The SRCP extended from 3 μm below the internal limiting membrane to 15 μm below the inner plexiform layer (IPL) and the DRCP extended from 15 to 70 μm below the IPL, as shown in Figure 1D, respectively.

Quantitative Analysis of OCT-A Images Based on Microvascular Density

Quantitative analysis of the vessel density at the levels of the SRCP and DRCP was performed using the en face OCT-A projection images (Fig. 1A1 for the superficial and Fig. 1A2 for the deep retinal capillary layers, respectively). A custom automated algorithm was used to quantify the microvascular density. The grayscale of each two-dimensional OCT-A image was first extended by bicubic interpolation to 1024 × 1024 pixels to enhance the image details. Then, the image was segmented to obtain the microvascular network. First, the boundary foveal avascular zone (FAZ) was detected by using a two-way combined method consisting of a canny edge detector algorithm and a level set algorithm. The area within the FAZ having a circle of fixed radius (diameter = 0.6 mm) was then determined to establish the baseline signal-to-noise ratio for the global thresholding.

The image was then processed separately to generate two binary images: the first one contained only the large blood vessels and was generated by using global thresholding, a local gray-level change enhancement algorithm called "gray-voting," Gabor filtering, and adaptive thresholding. The other binary image contained the large and small vessels and was created by using global thresholding, gray-voting algorithm, and adaptive thresholding. Last, the two resulting binary vessel maps were subtracted to obtain the binary image containing only the small vessels. Based on the final binary image, a skeletonized image was created by detecting the central axis of the binary, white-pixelated vasculature and remaining one pixel along the central axis.

Two forms of the analyzed regions were used to describe the density of the microvasculature. First, the density was calculated for the 2.5-mm-diameter total annular zone (TAZ) after excluding the FAZ (diameter = 0.6 mm, Figs. 1B1, 1B2). The density was also calculated in the four parafoveal quadrant sectors, that is, superior (S), temporal (T), inferior (I), and nasal (N) sectors of the 2.5-mm diameter circular zone after excluding the FAZ (Figs. 1C1, 1C2). The methods above were implemented using MATLAB v7.10 (MathWorks, Inc., Natick, MA, USA).

SD-OCT Procedure and Data Collection

The RTVue XR Avanti Spectral-Domain OCT system (Optovue, Inc.) with radial line scan was used to image the macular retina. All measurements were performed by a single, well-trained examiner. A radial scanning mode with 18 lines was applied to generate the 3D thickness maps (Fig. 2A). After SD-OCT image acquisition, data derived from the images were processed automatically by using a custom software to segment the eight intraretinal layers (Fig. 2C) as already described in our previously published articles.[21,22] Manual inspection and a few corrections were still required, especially in low-quality images. In the current study, the retina was divided into retinal nerve fiber layer (RNFL), ganglion cell layer and inner plexiform layer (GCIP), inner nuclear layer (INL), outer plexiform layer (OPL), Henle fiber layer and outer nuclear layer (HFL+ONL), myoid and ellipsoid zone (MEZ), outer segment of the photoreceptor cell (OS), and interdigitation zone and retinal pigment epithelium (IZ+RPE). For each eye included in this study, a 3D thickness map of the intraretinal layers in each eye was generated based on the segmented layers. For analysis, the macular thickness map was divided into nine sectors and was displayed in three concentric circles, including a central circular subfield (1-mm diameter), an internal ring (0.5–1.5 mm from the fovea), and an external ring (1.5–3.0 mm from the fovea) (Fig. 2B). The three

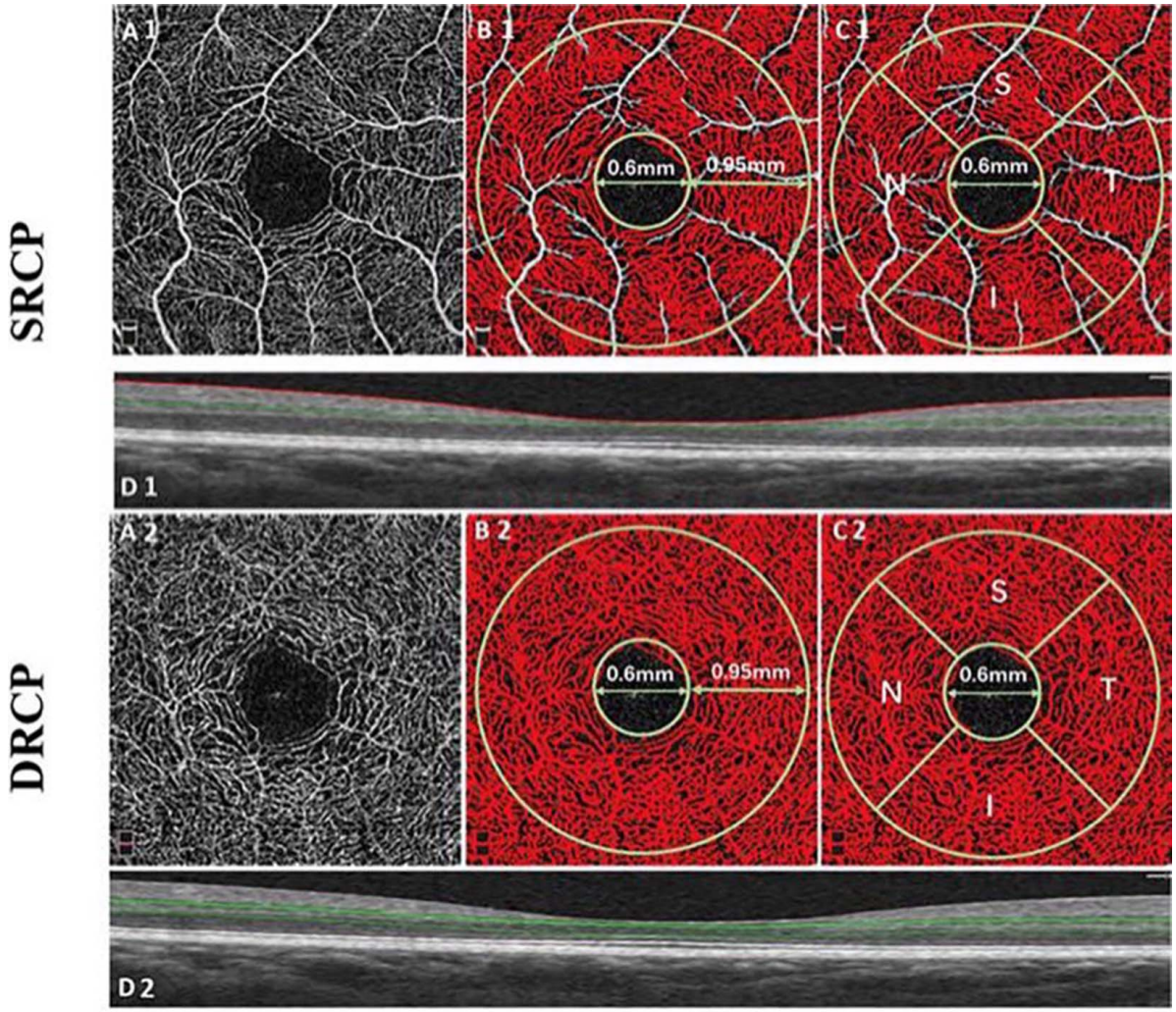

Figure 1. Representative OCT-A images and diagrammatic sketch showing the microvascular density analysis of the SRCP and DRCP. Original OCT-A images of both the SRCP (**A1**) and DRCP (**A2**). Binary images of the microvascular network after removing the large vessels with a width ≥25 μm and background noise in the SRCP (**B1**) and DRCP (**B2**). Microvascular density was performed on the TAZ with a diameter of 2.50 mm after excluding the FAZ (diameter = 0.60 mm) in both the SRCP (**B2**) and DRCP (**B2**). Images of the capillaries are shown with microvascular density performed in the parafoveal four quadrant sectors, S, T, I, and N, of a circular zone with a diameter of 2.50 mm after excluding the FAZ in the SRCP (**C1**) and DRCP (**C2**).

concentric areas were then divided into nine sectors, including the central (C) and S, I, T, and N regions of the internal ring (SI, II, TI, and NI, respectively) and the S, I, T, and N regions of the external ring (SE, IE, TE, and NE, respectively). The mean thickness for the total retinal in each sector was calculated.

Data Analysis and Statistical Methods

All statistical evaluation was done using SPSS software (version 17.0; SPSS Inc., Chicago, IL, USA). Data were expressed as mean ± SD. Refraction data were converted to SEs, calculated as the spherical dioptric power plus one-half of the cylindrical dioptric power. One-way ANOVA was used to test for the difference among the healthy controls and the PD group with post hoc tests used between the pair. Pearson correlation coefficients were calculated to assess correlations between the retinal structural parameter and microvascular density. $P < 0.05$ was considered to be statistically significant. Our data were adjusted for age and IOP. Generalized estimating equation was used to adjust the intercorrelation between two eyes with respect to intraretinal layer thickness and microvascular density.

Results

A total number of 49 eyes from 38 PD patients in their early stages and 34 eyes from 28 healthy controls were enrolled in this study. Twenty-seven eyes from PD patients and 22 healthy eyes were excluded due to SSI <40 or incompletion of OCT-A scans due to poor fixation. Demographics of the enrolled subjects are shown in Table 1. There was no statistical difference in the age and distribution of sex between the PD patients and the healthy controls. The difference between refractive error outcomes (spherical and astigmatic refractive error), axial length (AL), visual acuity (VA), body mass index (BMI), and mean arterial pressure (MAP) of the two groups was not statistically significant ($P > 0.05$). A significant difference was seen in the IOP between the two groups ($P < 0.05$). The average duration of the disease and treatment was 3.84 ± 2.80 years in patients with PD.

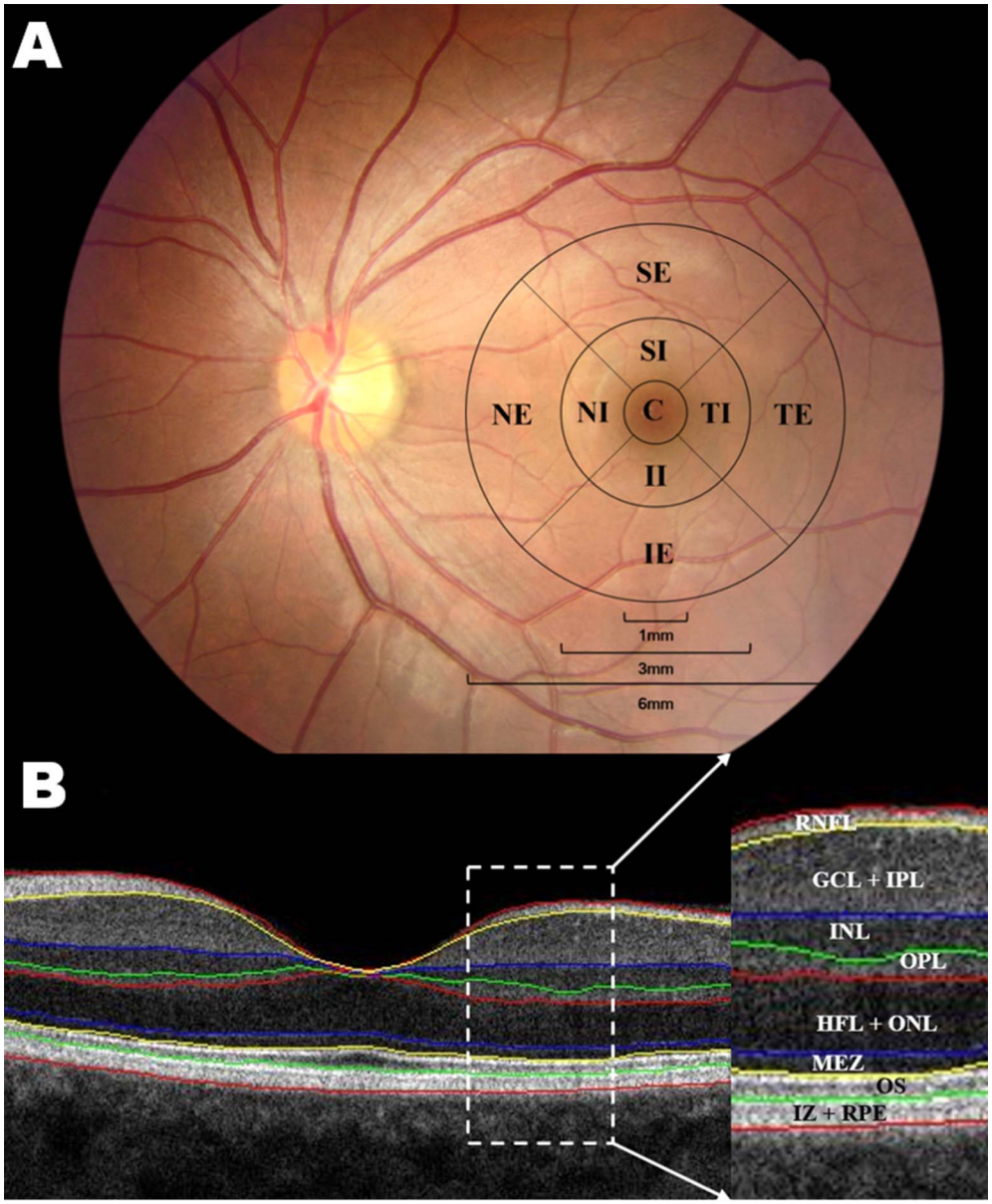

Figure 2. The intraretinal segmentation of the macula of a right eye. The radial scan model of the OCT-A and the nine regions around the macula (**A**). C, SI, II, TI, and NI regions of the internal ring and SE, IE, TE, and NE regions of the external ring. Automated segmentation of SD-OCT images (**B**) of a healthy subject; RNFL, GCIP, INL, OPL, HFL+ONL, MEZ, OS, and IZ+RPE.

Comparison of Microvascular Density Between Patients With PD and Healthy Controls

In the whole retinal capillary layer, microvascular density was significantly lower in the TAZ in PD patients when compared with the healthy controls ($P = 0.002$, Table 2). The SRCP was similar to that of the whole retinal layer where the microvascular density was significantly lower in the TAZ in PD patients when compared with the healthy controls ($P < 0.001$; Fig. 3, Table 2). There was no significant difference seen in the TAZ of the DRCP between PD patients and healthy controls ($P = 0.531$; Fig. 3, Table 2).

Quadrantal analyses showed significant microvascular loss occurred in most of the sectors (T, I, and N of the quadrant zones) in the whole retinal layer and all the quadrant sectors in the SRCP of the PD patients when compared with the healthy controls ($P < 0.05$; Fig. 3, Table 2). In the PD group, the

Table 1. General Systemic and Ophthalmologic Information in Patients With PD and Healthy Controls

	HC	PD	*P*
Age, y	61.18 ± 5.74	62.95 ± 7.97	0.180
MAP, mm Hg	92.98 ± 7.80	90.31 ± 6.99	0.483
Duration, y	–	3.84 ± 2.80	–
BMI	24.22 ± 3.45	23.02 ± 4.03	0.377
SE, D	0.77 ± 1.05	0.62 ± 1.96	0.616
BCVA, logMAR	0.97 ± 0.18	0.96 ± 0.23	0.958
AL, mm	23.16 ± 1.19	23.45 ± 0.78	0.155
IOP, mm Hg	9.32 ± 6.68	14.73 ± 2.75	<0.001*

Values are mean ± SD. BCVA, best corrected VA; HC, eyes of healthy controls; PD, eyes of patients with PD; SE, spherical equivalent.
* $P < 0.05$.

Table 2. Comparison of the Microvascular Density Between the PD Patients and Healthy Controls

	TAZ	S	T	I	N
SRCP					
HC	62.23 ± 3.31	61.91 ± 4.23	63.11 ± 4.12	61.76 ± 4.71	62.25 ± 3.81
PD	59.63 ± 2.95	59.66 ± 3.76	60.29 ± 3.92	59.10 ± 4.19	59.49 ± 4.05
*P**	<0.001	0.004	<0.001	0.002	<0.001
GEE*	0.002	0.001	0.002	0.002	0.005
DRCP					
HC	68.76 ± 5.26	69.76 ± 5.39	68.16 ± 5.46	69.88 ± 5.38	67.32 ± 6.29
PD	68.11 ± 5.43	68.92 ± 5.79	67.81 ± 4.98	68.99 ± 6.10	67.06 ± 6.13
*P**	0.531	0.446	0.730	0.428	0.829
GEE*	0.389	0.229	0.534	0.290	0.574
Whole retinal capillary plexus					
HC	61.21 ± 3.62	60.67 ± 4.21	61.74 ± 4.23	60.81 ± 5.06	61.68 ± 4.20
PD	59.44 ± 3.20	59.66 ± 4.10	60.28 ± 4.15	58.77 ± 4.29	59.09 ± 4.11
*P**	0.002	0.103	0.002	0.014	0.002
GEE*	0.002	0.081	0.002	0.001	0.002

GEE, generalized estimating equation.
* Adjusted for age and IOP.

microvascular density in both the superficial and deep capillary plexus did not significantly correlate with the disease severity using the H&Y scale and the duration ($P > 0.05$; Table 3).

Total and Intraretinal Macula Thickness

Compared with the healthy control group, the total thickness of the macula in the PD group was significantly thinner in the S, N, and I quadrants ($P < 0.05$; Fig. 3). The inner ring of the inferior sector of the RNFL was significantly thinner in PD patients when compared with the healthy controls ($P = 0.04$; Fig. 3). A significant thinning was shown in all but the temporal inner ring and the central region of GCIP layer in the eyes of the PD patients when compared with the healthy controls ($P < 0.05$; Fig. 3). The superior and inferior external ring of the INL was significantly thinner in the PD patients when both groups were compared ($P < 0.05$; Fig. 3). The HFL+ONL layer showed significant thinning in the superior and temporal external ring and the inferior internal ring ($P < 0.05$; Fig. 3). The nasal inner ring, S, and T quadrants of the OS layer showed significant thinning in the PD patients when compared with the healthy control ($P < 0.05$; Fig. 3). No significant correlation was shown between the average retinal thickness and the disease severity using the H&Y scale and the disease duration ($P > 0.05$; Table 4).

Association Between Retinal Structure and Microvascular Network

In PD patients, there was a positive correlation between the average GCIP thickness and the TAZ of the superficial microvascular density ($r = 0.249$, $P = 0.037$; Fig. 4). A positive correlation was also seen between the inner inferior thickness of the GCIP and inferior quadrant density ($r = 0.278$, $P = 0.019$; Fig. 4).

Discussion

In this study, we investigated the macular microvasculature evaluated with the SD-OCT-A and intraretinal layer thickness in PD patients in their early stages using SD-OCT. We have demonstrated the abnormalities of the microvascular density in PD, and found an association with GCIP thinning, suggesting that the microvascular abnormality, especially in the superficial capillary layer, may be associated with neurodegeneration. Our results indicate that OCT-A might provide a sensitive method for detecting microvascular changes in the early stages of PD, allowing the possibility of becoming a routine examination or screening.

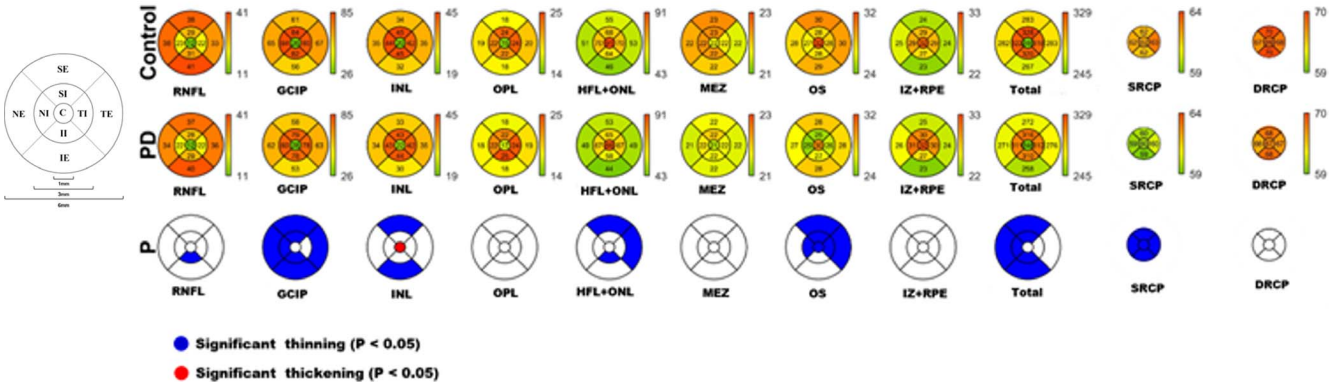

Figure 3. Comparison of the microvascular density and retinal thickness between patients with PD and healthy controls. The first two rows represent the retinal thickness maps and microvascular density of healthy controls and PD patients, respectively. The retinal thickness and microvascular density are indicated by the colors shown in the *color bar* for each row. The third row shows the corresponding parameters between the healthy controls and the PD patients; *blue* represents significant thinning ($P < 0.05$), *red* represents significant thickening ($P < 0.05$).

Table 3. Correlation Between Microvascular Density and the Severity of Disease Using the H&Y Scale and the Duration of PD

	TAZ	S	T	I	N
SRCP					
H&Y					
r	0.083	0.007	0.078	0.12	0.195
*P**	0.622	0.964	0.643	0.475	0.24
Duration, y					
r	−0.035	−0.136	−0.048	−0.09	−0.046
*P**	0.84	0.415	0.775	0.591	0.783
DRCP					
H&Y					
r	0.003	0.007	0.056	−0.026	−0.091
*P**	0.988	0.966	0.743	0.878	0.599
Duration, y					
r	0.117	0.015	0.031	0.003	0.028
*P**	0.491	0.931	0.857	0.987	0.870

* Adjusted for age and IOP.

Many studies have reported on the retinal degeneration in PD, particularly thinning of the RNFL and loss of ganglion cells.[23–25] However, just one article has reported on the retinal vascular abnormalities in PD.[26] OCT-A is a new advanced imaging technology that enables the noninvasive imaging of the retinal capillaries; it is especially useful for the in-depth analysis of retinal vessels in multiple layers that were previously invisible on the fundus images. To the best of our knowledge, this is the first study to report on the retinal microvascular abnormalities in PD patients using OCT-A. Our results demonstrated that the retinal capillary densities were significantly decreased in the early stages of PD when compared with the healthy control subjects with similar sex and age range, suggesting that the retinal capillary impairment occurs early in PD cascade before the clinically apparent motor disorders occur. Our results are compatible with earlier findings of ischemic events or vascular lesions in the PD group[27] and other neurological disorders.[28,29] Evidence from cross-sectional autopsy studies showed that cerebral small vessel disease has a relation with PD.[8,30] The retinal vasculature shares common characteristics with the brain vasculature[31,32]; therefore, our results may give evidence on the relationship of PD with cerebral small vessel disease.

Density reduction in the SRCP was found to be more significant than that in the DRCP in PD patients when compared with the healthy subjects. It is of interest to evaluate the possible pathophysiological basis of these results. Although cerebral dementia and neurodegeneration (particularly in forebrain) are the main hallmarks of PD, cerebral vascular changes are also known to occur in this disease. In particular, vascular degeneration was evident in multiple brain regions, such as the substantia nigra in postmortem cases of PD with disruption of the endothelium as well.[9] Given the homology between the retinal and cerebral microvasculature, concomitant cerebral angiopathy in PD might extend to the retina, resulting in changes to microvascular network. Additionally, previous reports on the retinal live imaging of animal models with PD detected α-synuclein along the wall of the blood vessels and more prominently in the arteries[33] that are located in the superficial layer of the retina, responsible for the arterial side of circulation.[34] That may help to explain why we found microvascular density decreased more in the superficial vascular layer rather than that in the deep vascular layer in the current study.

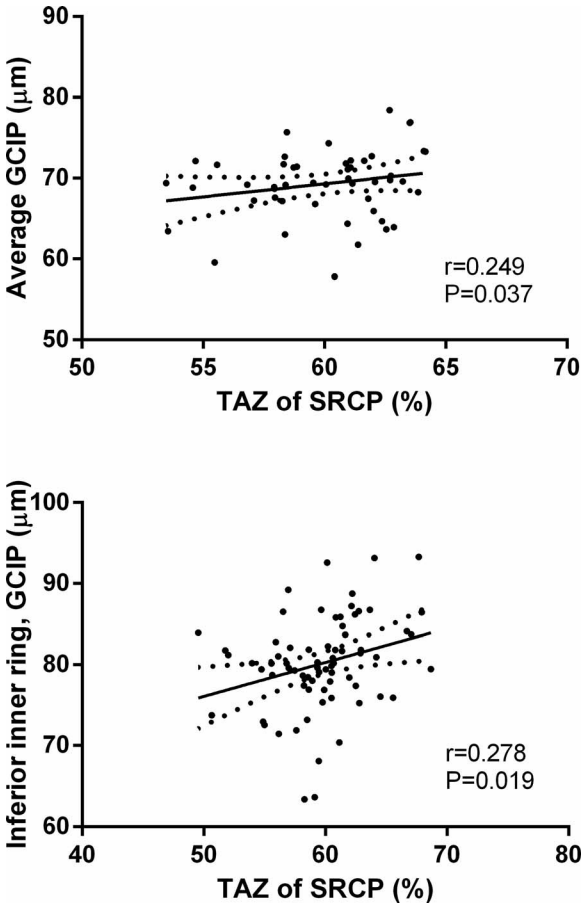

Figure 4. Correlation of microvascular density and retina thickness in PD. Correlation of average GCIP thickness and TAZ of SRCP (*top*). Correlation of inferior ring of GCIP thickness and TAZ of SRCP (*bottom*).

We did not find any relationship of disease duration or disease severity with retinal microvascular densities or intraretinal layer thickness. This is in line with results of some previous OCT measures, showing no association of RNFL, total macular volume, or intraretinal layer thickness with disease severity or duration.[35–37] The possible explanations for this result may be because of the study population, which

Table 4. Correlation Between Average Macular Thickness and the Severity of Disease Using the H&Y Scale and the Duration of PD

Average Thickness	RNFL	GCIP	INL	OPL	ONL	OS	IZ+RPE	Total Macular
H&Y								
r	−0.077	−0.12	−0.095	−0.093	−0.273	0.092	−0.077	−0.216
*P**	0.617	0.466	0.535	0.542	0.097	0.548	0.654	0.22
Duration, y								
r	0.086	−0.147	−0.245	0.022	−0.296	0.03	−0.266	−0.301
*P**	0.574	0.373	0.105	0.887	0.071	0.845	0.117	0.84

* Adjusted for age and IOP.

comprises a high proportion of PD patients in their early stages. Even so, we found an important correlation between microvascular density in the superficial vascular layer and GCIP measured by OCT; the positive correlation with the GCIP demonstrated that patients with lower microvascular density in the superficial vascular layer tend to have more GCIP thinning. The GCIP thinning reflected the neurodegeneration, as previous studies reported.[35,38] Our results indicate that retinal microvascular abnormality may contribute to the neurodegenerative progression. Longitudinal studies with a large sample size are needed to obtain statistically reliable associations regarding changes of retinal microvascular densities and clinical features of PD patients to further determine the clinical specificity of OCT-A measures.

There are several limitations to the current study. First, the IOP in PD patients was significantly higher than in the healthy participants, although it was within the normal range (<21 mm Hg). For this reason, all analyses were adjusted for IOP. Second, selecting hospital staff as our control group is another limitation of this study, as they may not be from the same socioeconomic status or have the same diet as our PD group, and thus may affect our data. Also, two eyes from some of the same subjects (both PD and healthy controls, respectively) were included in this current study; these types of data may characteristically inflate the sample size. Another important limitation is that the field of view from the current OCT-A systems is small, which restricts imaging to the posterior pole. Development of higher-speed OCT systems capable of wide-field OCT-A scans will ease this limitation. Despite the presence of the algorithm to reduce motion artifacts, 6 PD patients and 2 healthy control subjects still had motion artifacts in the deep capillary plexus owing to the patients' eye movements and were excluded from our data. Given that this technology is still developing, further enhancement and refinement of the software are essential to improve its reproducibility and usability for more neurovascular diseases in the future. Also, improvement of processing algorithms will be needed to reduce these artifacts and improve the reliability of microvascular density, microvascular area, and flow measurements. The current OCT-A assesses vascular flow only within a limited range of dynamic velocity.[39] The ability of OCT-A to visualize blood flow is restricted to a definite range of flow velocities (minimum 0.5–2.0 mm/s; saturation 9.0 mm/s estimated for current devices). Also, the decorrelation values produced by the split-spectrum amplitude-decorrelation angiography (SSADA) saturates at velocity levels larger than capillaries; thus, the flow index is likely to miscalculate blood flow changes. Moreover, capillary diameters (5–10 μm) are generally finer than the transverse resolution of the OCT beam (~15 μm), the SSADA vessel density index is likely to overestimate actual vessel density while underestimating change. This may be resolved by a more sensitive algorithm to detect very low velocity using swept-light source OCT angiography. Finally, due to the cross-sectional, noninterventional design of the study, it was not possible to evaluate the potentially confounding impact of PD medications (cumulative levodopa dose and the homocysteine plasma levels) on vascular measurements. All PD patients were treated using levodopa (all patients) at the time of OCT-A imaging. Therefore, we could not rule out the impact of systemic medications on microvascular density measurements. Further studies are needed to address the influence of PD drug therapy on OCT-A measurements.

In conclusion, our results indicated that retinal microvascular density decreased in PD patients. The correlation between microvascular impairment in the superficial retinal capillary layer and GCIP thinning also revealed that the retinal microvascular abnormality may contribute to the neurodegeneration in PD patients. Although we cannot verify if PD is a direct consequence of small vessel disease or just a coincident finding, our results nonetheless suggest that OCT-A measurement of the retinal microvascular network with quantitative analysis may be a potential adjunct to detect vascular changes in the early stages of PD and provide a new imaging target for early diagnosis and management of PD.

Acknowledgments

Supported by research grants from the National Nature Science Foundation of China (Grant Nos. 81570880 and11675122), the National Key Research and Development Program of China (2016YFE0107000, 2016YFC0102500), 111 Project (D16011), Zhejiang Provincial Natural Science Foundation of China (Grant No. LY16H160047), and Public Service Program of Wenzhou Science and Technology Bureau (Y20160151).

Disclosure: **W.R. Kwapong**, None; **H. Ye**, None; **C. Peng**, None; **X. Zhuang**, None; **J. Wang**, None; **M. Shen**, None; **F. Lu**, None

References

1. Calne DB, Zigmond MJ. Compensatory mechanisms in degenerative neurologic diseases. Insights from parkinsonism. *Arch Neurol*. 1991;48:361–363.
2. Khoo TK, Yarnall AJ, Duncan GW, et al. The spectrum of nonmotor symptoms in early Parkinson disease. *Neurology*. 2013;80:276–281.
3. Kwon DH, Kim JM, Oh SH, et al. Seven-Tesla magnetic resonance images of the substantia nigra in Parkinson disease. *Ann Neurol*. 2012;71:267–277.
4. Hajee ME, March WF, Lazzaro DR, et al. Inner retinal layer thinning in Parkinson disease. *Arch Ophthalmol*. 2009;127:737–741.
5. Bodis-Wollner I, Kozlowski PB, Glazman S, Miri S. Alpha-synuclein in the inner retina in Parkinson disease. *Ann Neurol*. 2014;75:964–966.
6. Archibald NK, Clarke MP, Mosimann UP, Burn DJ. Visual symptoms in Parkinson's disease and Parkinson's disease dementia. *Mov Disord*. 2011;26:2387–2395.
7. Armstrong RA. Visual symptoms in Parkinson's disease. *Parkinsons Dis*. 2011;2011:908306.
8. Schwartz RS, Halliday GM, Cordato DJ, Kril JJ. Small-vessel disease in patients with Parkinson's disease: a clinicopathological study. *Mov Disord*. 2012;27:1506–1512.
9. Guan J, Pavlovic D, Dalkie N, et al. Vascular degeneration in Parkinson's disease. *Brain Pathol*. 2013;23:154–164.
10. Ruck T, Bittner S, Meuth SG. Blood-brain barrier modeling: challenges and perspectives. *Neural Regen Res*. 2015;10:889–891.
11. MacCormick IJ, Czanner G, Faragher B. Developing retinal biomarkers of neurological disease: an analytical perspective. *Biomark Med*. 2015;9:691–701.
12. Garcia-Martin E, Ara JR, Martin J, et al. Retinal and optic nerve degeneration in patients with multiple sclerosis followed up for 5 years. *Ophthalmology*. 2017;124:688–696.
13. Manogaran P, Hanson JV, Olbert ED, et al. Optical coherence tomography and magnetic resonance imaging in multiple sclerosis and neuromyelitis optica spectrum disorder. *Int J Mol Sci*. 2016;15:E1894.
14. Chhablani PP, Ambiya V, Nair AG, Bondalapati S, Chhablani J. Retinal findings on OCT in systemic conditions. *Semin Ophthalmol*. 2018;33:525–546.
15. Kirbas S, Turkyilmaz K, Tufekci A, Durmus M. Retinal nerve fiber layer thickness in Parkinson disease. *J Neuroophthalmol*. 2013;33:62–65.
16. Lee JY, Kim JM, Ahn J, Kim HJ, Jeon BS, Kim TW. Retinal nerve fiber layer thickness and visual hallucinations in Parkinson's Disease. *Mov Disord*. 2014;29:61–67.

17. Aaker GD, Myung JS, Ehrlich JR, Mohammed M, Henchcliffe C, Kiss S. Detection of retinal changes in Parkinson's disease with spectral-domain optical coherence tomography. *Clin Ophthalmol*. 2010;4:1427–1432.
18. Reichmann H. Clinical criteria for the diagnosis of Parkinson's disease. *Neurodegener Dis*. 2010;7:284–290.
19. Hoehn MM, Yahr MD. Parkinsonism: onset, progression, and mortality. 1967. *Neurology*. 2001;57:S11–S26.
20. Spaide RF, Klancnik JM Jr, Cooney MJ. Retinal vascular layers imaged by fluorescein angiography and optical coherence tomography angiography. *JAMA Ophthalmol*. 2015;133:45–50.
21. Cheng D, Wang Y, Huang S, et al. Macular inner retinal layer thickening and outer retinal layer damage correlate with visual acuity during remission in Behcet's disease. *Invest Ophthalmol Vis Sci*. 2016;57:5470–5478.
22. Liu X, Shen M, Yuan Y, et al. Macular thickness profiles of intraretinal layers in myopia evaluated by ultrahigh-resolution optical coherence tomography. *Am J Ophthalmol*. 2015;160:53–61.e2.
23. Albrecht P, Muller AK, Sudmeyer M, et al. Optical coherence tomography in parkinsonian syndromes. *PLoS One*. 2012;7:e34891.
24. Balk LJ, Petzold A, Oberwahrenbrock T, Brandt AU, Albrecht P. Distribution of retinal layer atrophy in patients with Parkinson disease and association with disease severity and duration. *Am J Ophthalmol*. 2014;158:845.
25. Garcia-Martin E, Larrosa JM, Polo V, et al. Distribution of retinal layer atrophy in patients with Parkinson disease and association with disease severity and duration. *Am J Ophthalmol*. 2014;157:470–478.e2.
26. Kromer R, Buhmann C, Hidding U, et al. Evaluation of retinal vessel morphology in patients with Parkinson's disease using optical coherence tomography. *PLoS One*. 2016;11:e0161136.
27. Song IU, Lee JE, Kwon DY, Park JH, Ma HI. Parkinson's disease might increase the risk of cerebral ischemic lesions. *Int J Med Sci*. 2017;14:319–322.
28. Kalaria RN. The role of cerebral ischemia in Alzheimer's disease. *Neurobiol Aging*. 2000;21:321–330.
29. Alavi A, Clark C, Fazekas F. Cerebral ischemia and Alzheimer's disease: critical role of PET and implications for therapeutic intervention. *J Nucl Med*. 1998;39:1363–1365.
30. Abe K. Cerebral small vessel disease and incident parkinsonism: the RUN DMC study. *Neurology*. 2016;86:1268–1269.
31. Erskine L, Herrera E. Connecting the retina to the brain. *ASN Neuro*. 2014;6:e1759091414562107.
32. London A, Benhar I, Schwartz M. The retina as a window to the brain—from eye research to CNS disorders. *Nat Rev Neurol*. 2013;9:44–53.
33. Price DL, Rockenstein E, Mante M, et al. Longitudinal live imaging of retinal alpha-synuclein::GFP deposits in a transgenic mouse model of Parkinson's disease/dementia with Lewy bodies. *Sci Rep*. 2016;6:29523.
34. Iwasaki M, Inomata H. Relation between superficial capillaries and foveal structures in the human retina. *Invest Ophthalmol Vis Sci*. 1986;27:1698–1705.
35. Sari ES, Koc R, Yazici A, Sahin G, Ermis SS. Ganglion cell-inner plexiform layer thickness in patients with Parkinson disease and association with disease severity and duration. *J Neuroophthalmol*. 2015;35:117–121.
36. Aaker GD, Myung JS, Ehrlich JR, Mohammed M, Henchcliffe C, Kiss S. Detection of retinal changes in Parkinson's disease with spectral-domain optical coherence tomography. *Clin Ophthalmol*. 2010;4:1427–1432.
37. Roth NM, Saidha S, Zimmermann H, et al. Photoreceptor layer thinning in idiopathic Parkinson's disease. *Mov Disord*. 2014;29:1163–1170.
38. Zivkovic M, Dayanir V, Stamenovic J, et al. Retinal ganglion cell/inner plexiform layer thickness in patients with Parkinson's disease. *Folia Neuropathol*. 2017;55:168–173.
39. Jia Y, Tan O, Tokayer J, et al. Split-spectrum amplitude-decorrelation angiography with optical coherence tomography. *Opt Express*. 2012;20:4710–4725.

Investigative Ophthalmology & Visual Science